

# Recovery rates reflect distance to a tipping point in a living system

Annelies J. Veraart<sup>1</sup>, Elisabeth J. Faassen<sup>1</sup>, Vasilis Dakos<sup>1</sup>, Egbert H. van Nes<sup>1</sup>, Miquel Lürling<sup>1,2</sup> & Marten Scheffer<sup>1</sup>

**Tipping points, at which complex systems can shift abruptly from one state to another, are notoriously difficult to predict<sup>1</sup>. Theory proposes that early warning signals may be based on the phenomenon that recovery rates from small perturbations should tend to zero when approaching a tipping point<sup>2,3</sup>; however, evidence that this happens in living systems is lacking. Here we test such ‘critical slowing down’ using a microcosm in which photo-inhibition drives a cyanobacterial population to a classical tipping point when a critical light level is exceeded. We show that over a large range of conditions, recovery from small perturbations becomes slower as the system comes closer to the critical point. In addition, autocorrelation in the subtle fluctuations of the system’s state rose towards the tipping point, supporting the idea that this metric can be used as an indirect indicator of slowing down<sup>4,5</sup>. Although stochasticity prohibits prediction of the timing of critical transitions, our results suggest that indicators of slowing down may be used to rank complex systems on a broad scale from resilient to fragile.**

Systems ranging from the brain and society to ecosystems and the climate can have tipping points at which minor perturbations can invoke a critical transition to a contrasting state<sup>6</sup>. The complexity of such systems prohibits accurate predictive modelling. However, it has been suggested that even without mechanistic insight, the proximity of a tipping point may be inferred from generic features of fluctuations and spatial patterns that can be interpreted as early warning indicators<sup>1,7–9</sup>. This idea is based on the phenomenon that at bifurcation points at which stability of an equilibrium changes, the dominant real eigenvalue becomes zero<sup>10</sup>. As a result, the rate of recovery from perturbation should go to zero as such bifurcations are approached (Supplementary Notes 1). This phenomenon, which is known as critical slowing down, is well established in physics but it has only recently been suggested that the recovery rate from perturbations could be an indicator of the distance to a tipping point in complex living systems such as ecosystems<sup>3</sup>.

Although the prospect that the fragility of living systems could be probed this way is attractive, experimental evidence has so far been lacking. Instead, much work has been focused on ways to infer slowing down from indirect indicators such as autocorrelation and variance. However, although these indicators are linked to slowing down in simple stochastically forced models<sup>1,5,9</sup>, recent theoretical studies indicate that the indirect indicators will not always respond in simple ways<sup>11</sup> (Brock, W. A. & Carpenter, S. R., submitted). This is confirmed by empirical studies on the climate<sup>5</sup>, the food web of a lake<sup>12</sup> and laboratory populations of water fleas<sup>13</sup>. In these systems, trends in indirect indicators occurred but were not all consistent. Here we use a controlled system in which there is positive feedback between organisms and their physical environment to test critical slowing down directly from recovery rates.

We exposed cyanobacteria in chemostat microcosms to increasing light stress. This is a well understood system for which models have shown alternative stable states and tipping points<sup>14,15</sup>. Cyanobacteria provide the shade needed for their own growth, creating a positive feedback, and this constitutes the mechanism behind the bistability.

Although light is needed for photosynthesis, light levels that are too high are detrimental to primary producers such as the cyanobacteria that we used. Mutual shading can ameliorate this stress, and is thus one of the ways in which facilitation can outweigh competitive interactions under harsh conditions<sup>16</sup>. Such feedback between organisms and their environment is the mechanism behind alternative stable states in a range of ecosystems<sup>17</sup>. Indeed, as a result of the facilitative shading, our system can maintain a high biomass under incident light levels that prohibit growth in low biomass cultures. A fold bifurcation that represents a classical tipping point occurs at the light level at which this mechanism becomes too weak to allow persistence of the population<sup>14,15</sup> (see Supplementary Notes 1 for a model analysis). Here, shading becomes insufficient to prevent growth inhibition, and the resulting loss of biomass further weakens the stabilizing shading effect. This implies that a positive feedback is driving the system towards a crash.

We cultured cyanobacteria in two independently controlled chemostat microcosms (M1 and M2) and increased incident light daily in small steps to the point at which the population collapsed (see Methods). We perturbed the populations every 4–5 days by removing 10% of their biomass through dilution. Consistent with the model results (Supplementary Fig. 1.1) the populations maintained a relatively high biomass throughout the experiment until they collapsed rather markedly when a tipping point was reached (Fig. 1 and Supplementary Notes 3). Recovery rates of both systems decreased gradually

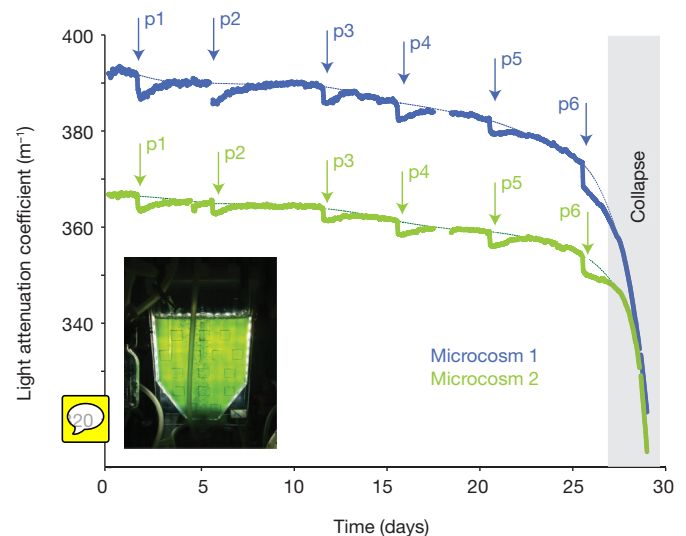


**Figure 1 | The response of two populations of cyanobacteria (*Aphanizomenon flos-aquae*) to dilution events under a regime of gradually increasing light levels.** Dilution events are indicated as perturbations p1–p6. The light attenuation coefficient is a measure of population density. Thin curve segments represent the baselines that were used for computing recovery rates. The inset shows the experimental system.

<sup>1</sup>Department of Aquatic Ecology and Water Quality Management, Wageningen University, PO Box 47, NL-6700 AA, Wageningen, The Netherlands. <sup>2</sup>Department of Aquatic Ecology, Netherlands Institute of Ecology, Royal Netherlands Academy of Arts and Sciences, PO Box 50, 6700AB, Wageningen, The Netherlands.

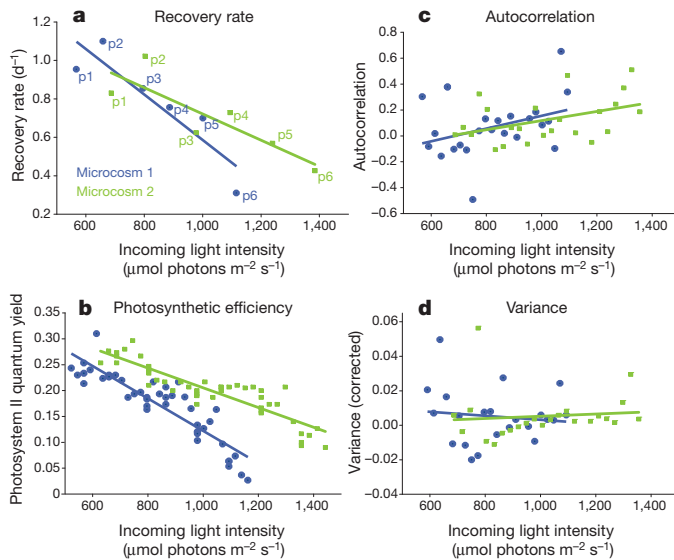


**Figure 2 | Indicators of slowing down as a function of light intensity.** **a**, Recovery rates after perturbation (p1–p6). **b**, Photosynthetic efficiency (photosystem II quantum yield). **c**, Autocorrelation in the population density estimator for each day based on 30 min average  $I_{out}$  data. **d**, Corrected variance in daily time series (see Methods and Supplementary Notes 4). Fisher's combined (one-tailed) significance test of the slopes of the regression line's ( $n = 6$ ) in both microcosms: recovery rate,  $\chi^2_4 = 18.48$ ,  $P = 0.001$  (if the p6 perturbations are excluded ( $n = 5$ ),  $\chi^2_4 = 12.39$ ,  $P = 0.015$ ); photosynthetic efficiency  $n = 45$ ,  $\chi^2_4 = 147.66$ ,  $P < 0.001$ ; autocorrelation,  $n = 23$ ,  $\chi^2_4 = 14.00$ ,  $P = 0.007$ ; variance, not significant,  $n = 23$ ,  $\chi^2_4 = 7.72$ ,  $P = 0.102$ .

towards the tipping point, starting far from the bifurcation (Fig. 2a), and tended to decline more rapidly towards the tipping point. This was also predicted by our model (Supplementary Fig. 1.1).

In most complex systems, the mechanisms that are involved in causing the slowing down will be difficult to unravel. However, in our particular system the photosynthetic capacity of the cyanobacteria that is at the heart of their growth potential can be sensed through measurements of the efficiency of their light harvesting system (see Methods). Whereas biomass remained relatively high in the trajectory towards the critical threshold, this specific indicator of their vigour declined linearly with increasing light stress, approaching zero at the point of collapse (Fig. 2b). This is an independent confirmation that the light-induced stress to the cyanobacteria in the two independently operated microcosms does indeed undermine the resilience of the system to the point at which collapse is inevitable.

In systems that are subject to stochastic perturbation regimes, slowing down is predicted to be reflected in characteristic changes in fluctuations of the state. In particular, it has been proposed that increases in autocorrelation and variance can be interpreted as indirect indicators of slowing down<sup>1,4,9</sup>. Although our experiment was not primarily designed to study the effect of stochastic perturbation regimes, there are continuous subtle fluctuations in our measurements of the density of the cyanobacterial population. These fluctuations will reflect a mixture of factors including measurement noise and instabilities in the lighting system as well as true population fluctuations induced by the slightly fluctuating conditions in the bubbled microcosms. We studied how autocorrelation and variance in these subtle fluctuations changed as our system approached the critical point. For this we analysed all the stretches of continuous measurements of 1 day between the experimental interruptions caused by the daily stepwise increase of light intensity and the dilution perturbation events (see Methods). Although autocorrelation was quite variable in the time series that we studied, there was a significant increase towards the tipping point in both experimental systems (Fig. 2c). No trend in variance was apparent in the systems (Fig. 2d, see also Supplementary Notes 4).

These results are consistent with the prediction that measuring recovery rates from perturbations is a robust way to detect critical slowing down<sup>18</sup>, whereas indirect indicators of slowing down may or may not increase towards a critical threshold<sup>11</sup>. Also, our findings are consistent with the prediction that autocorrelation is usually directly related to slowing down and may therefore provide a more robust signal than variance in some situations<sup>11</sup>.

Perturbation experiments such as the ones in our experiment will often be impossible in large complex systems, leaving indirect indicators as the only tool by which to infer slowing down. However, experimental probing of recovery rates may be feasible in some smaller systems, as long as the timescales are appropriate and stochastic fluctuations are small relative to experimental perturbations. Even in larger systems, local perturbations may be an option to probe resilience, allowing adaptive management to steer the system away from the brink of collapse.

Perhaps most importantly, our experimental demonstration of slowing down implies a proof of concept, providing a fundamental basis to the current search for generic early warning signals in systems ranging from the brain and ecosystems to society and the climate<sup>1</sup>. The fact that slowing down in our system started far from the critical point suggests that recovery rates as well as indirect indicators may be used to rank such complex systems on a broad scale from stable to critical. This does not mean that slowing down can be used to actually predict transitions. Stochastic shocks will trigger critical transitions always before the bifurcation point is reached, indicating that there is inherent unpredictability in systems. Nevertheless, the prospect of having generic indicators of resilience is a potentially large step forward. Mechanistic models to predict tipping points in nature and society accurately are simply beyond our reach, leaving empirical estimation of fragility as one of the key challenges in complex systems science today<sup>1</sup>.

## METHODS SUMMARY

Experiments were performed in two identical flat chemostat microcosms<sup>19</sup> (M1 and M2) in which we cultured cyanobacteria (*Aphanizomenon flos-aquae* (L.) Ralfs) on a nutrient-rich growth medium, modified from BG11 medium<sup>20</sup>. Light irradiance was increased in steps of 23  $\mu\text{mol photons m}^{-2} \text{s}^{-1}$  for M1 and 29  $\mu\text{mol photons m}^{-2} \text{s}^{-1}$  each day for M2. Photosynthetic efficiency was measured from diurnal samples. The intensity of the light passing through the chemostats was averaged at 5-min intervals, and light attenuation coefficients ( $\epsilon$ ,  $\text{m}^{-1}$ ) were calculated as an indicator of biomass:

$$\epsilon = \frac{-\ln(I_{out}/I_{in})}{d}$$

where  $I_{in}$  is the intensity of the incoming light ( $\mu\text{E}$ ),  $I_{out}$  is the intensity of the outgoing light ( $\mu\text{E}$ ) and  $d$  is the depth of the chemostats (m). External perturbations were performed every 4–5 days by diluting the culture with 170 ml of sterile medium. A baseline for calculating recovery rates was constructed for each perturbation event (Supplementary Notes 2 and Supplementary Fig. 2.1) by fitting a quadratic curve from the period just before perturbation to the period just before the next perturbation (thin curves in Fig. 1). Recovery rates after each perturbation ( $\lambda$ , per day) were then calculated from a linear regression of  $-\ln(\epsilon_0 - \epsilon_c)$  against time, where  $\epsilon_0$  is the light attenuation of the baseline ( $\text{m}^{-1}$ ) and  $\epsilon_c$  is the light attenuation of the chemostat ( $\text{m}^{-1}$ )<sup>3</sup>.

The lag 1 autocorrelation and variance were analysed for each uninterrupted period between the daily manipulations after removing the trends from each period by fitting polynomials of 2 degrees. To check for effects of nonlinear propagation of measurement noise, we constructed a null model that assumed that all residuals were due to uncorrelated normally distributed noise. As variance showed a trend towards the bifurcation in this null model (Supplementary Table 4.1), we corrected the observed variance by subtracting the median of the null model (Fig. 2d).

**Full Methods** and any associated references are available in the online version of the paper at [www.nature.com/nature](http://www.nature.com/nature).

Received 13 September; accepted 18 November 2011.

Published online 25 December 2011.

- Scheffer, M. *et al.* Early-warning signals for critical transitions. *Nature* **461**, 53–59 (2009).

2. Wissel, C. A universal law of the characteristic return time near thresholds. *Oecologia* **65**, 101–107 (1984).
3. van Nes, E. H. & Scheffer, M. Slow recovery from perturbations as a generic indicator of a nearby catastrophic shift. *Am. Nat.* **169**, 738–747 (2007).
4. Ives, A. R. Measuring resilience in stochastic systems. *Ecol. Monogr.* **65**, 217–233 (1995).
5. Dakos, V. *et al.* Slowing down as an early warning signal for abrupt climate change. *Proc. Natl Acad. Sci. USA* **105**, 14308–14312 (2008).
6. Scheffer, M. *Critical Transitions in Nature and Society* (eds Levin, S.A. & Strogatz, S.H.) (Princeton Univ. Press, 2009).
7. Kleinen, T., Held, H. & Petschel-Held, G. The potential role of spectral properties in detecting thresholds in the Earth system: application to the thermohaline circulation. *Ocean Dyn.* **53**, 53–63 (2003).
8. Held, H. & Kleinen, T. Detection of climate system bifurcations by degenerate fingerprinting. *Geophys. Res. Lett.* **31**, L23207 (2004).
9. Carpenter, S. R. & Brock, W. A. Rising variance: a leading indicator of ecological transition. *Ecol. Lett.* **9**, 311–318 (2006).
10. Strogatz, S. H. *Nonlinear Dynamics and Chaos: With Applications to Physics, Biology, Chemistry and Engineering* 1st edn (Addison-Wesley, 1994).
11. Dakos, V., van Nes, E. H., D'Odorico, P. & Scheffer, M. How robust are variance and autocorrelation as early-warning signals for critical transitions? *Ecology* (submitted); preprint at <http://dx.doi.org/10.1890/11-0889.1>.
12. Carpenter, S. R. *et al.* Early warnings of regime shifts: A whole-ecosystem experiment. *Science* **332**, 1079–1082 (2011).
13. Drake, J. M. & Griffen, B. D. Early warning signals of extinction in deteriorating environments. *Nature* (2010).
14. Huisman, J. *The Struggle for Light*. PhD thesis, Univ. Groningen (1997).
15. Gerla, D. J., Mooij, W. M. & Huisman, J. Photoinhibition and the assembly of light-limited phytoplankton communities. *Oikos* **120**, 359–368 (2011).
16. Holmgren, M., Scheffer, M. & Huston, M. A. The interplay of facilitation and competition in plant communities. *Ecology* **78**, 1966–1975 (1997).
17. Scheffer, M., Carpenter, S. R., Foley, J. A., Folke, C. & Walker, B. Catastrophic shifts in ecosystems. *Nature* **413**, 591–596 (2001).
18. Dakos, V., Kéfi, S., Rietkerk, M., van Nes, E. H. & Scheffer, M. Slowing down in spatially patterned ecosystems at the brink of collapse. *Am. Nat.* **177**, E153–E166 (2011).
19. Huisman, J. *et al.* Principles of the light-limited chemostat: theory and ecological applications. *Antonie Leeuwenhoek* **81**, 117–133 (2002).
20. Andersen, R. A., Berges, J.A., Harrison, P.J. & Watanabe M.M. in *Algal culturing techniques* 1st edn 435–436 (Elsevier, 2005).

**Supplementary Information** is linked to the online version of the paper at [www.nature.com/nature](http://www.nature.com/nature).

**Acknowledgements** We thank M. B. Gonçalves Souza for discussions on the experimental set up. We thank D. Waasdorp and W. Beekman-Lukassen for assistance with the experiments and C. ter Braak for statistical advice. A.J.V., E.J.F., V.D., E.H.v.N. and M.S. are supported by a European Research Council Advanced grant and M.S. is the recipient of a Spinoza award.

**Author Contributions** A.J.V., E.J.F. and M.L. performed the experiments. A.J.V., E.J.F., E.H.v.N. and V.D. analysed the data. M.S., A.J.V., E.H.v.N., E.J.F. and V.D. wrote the paper. All authors discussed the results and commented on the manuscript.

**Author Information** Reprints and permissions information is available at [www.nature.com/reprints](http://www.nature.com/reprints). The authors declare no competing financial interests. Readers are welcome to comment on the online version of this article at [www.nature.com/nature](http://www.nature.com/nature). Correspondence and requests for materials should be addressed to E.H.v.N. ([egbert.vannes@wur.nl](mailto:egbert.vannes@wur.nl)).

## METHODS

**Experimental conditions.** Experiments were performed in two identical flat chemostats (V 1.7 l, 0.05 m optical path length)<sup>19</sup>. In these chemostats we cultured the cyanobacterium *Aphanizomenon flos-aquae* (L.) Ralfs on a nutrient-rich sterile growth medium that was modified from BG11 medium<sup>20</sup>. The chemostats were kept at a stable temperature of 21 °C. A continuous flow of moistened air of 60–100 ml min<sup>-1</sup> was supplied through a sintered glass sieve at the bottom of the vessel to ensure homogenous mixing of the culture. The air was mixed with CO<sub>2</sub> to satisfy the inorganic carbon need of the culture. CO<sub>2</sub> flow was adjusted, when needed, to maintain a pH of between 7.1 and 8.1. The chemostats were run at a dilution rate of 0.18 per day for chemostat 1 (named M1) and 0.21 per day for chemostat 2 and (M2). They were illuminated using white LED lamps (SL3500w, Photon Systems Instruments). Light irradiance was increased by 23 μmol photons m<sup>-2</sup> s<sup>-1</sup> per day for M1 and 29 μmol photons m<sup>-2</sup> s<sup>-1</sup> per day for M2 by a Light Studio 1.3 12C interface (Photon Systems Instruments, Brno).

**Daily maintenance and measurements.** Each day the walls of the chemostats were scraped with a magnetic stirrer to prevent cyanobacterial attachment. After scraping, we took samples to determine chlorophyll *a* concentrations and photosystem II quantum yield (in triplicate) using a PhytoPAM (phyto-ED), and to determine biovolume in a 400-μl sample volume (in triplicate) using a Casy TT Cell Counter, with a 150-μm capillary (Innovatis AG Casy Technology). The intensity of the light penetrating through the chemostat was recorded continuously using RA100 light sensors (Bottemanne Weather Instruments) that were attached to the outer wall of the chemostat and stored as 5-min averages on Squirell SQ1000 dataloggers (Grant Instruments). The light sensors were removed during scraping of the chemostats.

**Perturbations.** At an incoming light intensity of 477 μmol photons m<sup>-2</sup> s<sup>-1</sup> for M1 and 571 for M2, the light attenuation coefficients of the chemostats became stable. From this moment on, perturbations were performed every 4–5 days by diluting the culture with 170 ml of sterile medium. The dilution was always performed 2 h after the daily stepwise increase in light.

**Recovery rates.** We used the calculated light attenuation (Fig. 1 and Supplementary Note 2) as a measure of the cyanobacterial biomass<sup>21</sup>. Before calculation of recovery rates, the light data were corrected for sensor attachment differences (Supplementary Note 2). Vertical light attenuation ( $\varepsilon$ , m<sup>-1</sup>) was calculated from the corrected light data:

$$\varepsilon = \frac{-\ln(I_{\text{out}}/I_{\text{in}})}{d}$$

where  $I_{\text{in}}$  is the intensity of the incoming light,  $I_{\text{out}}$  is the intensity of the outgoing light (both measured in μmol photons m<sup>-2</sup> s<sup>-1</sup>) and  $d$  is the optical path length of the chemostats (m). Light attenuation data were smoothed for calculation of recovery rates by taking a moving average of 1 h.

To calculate recovery rates, a baseline was constructed for each perturbation event. This baseline was obtained by fitting a quadratic curve from the period just before perturbation to the period just before the next perturbation (Fig. 1). Parameters for the baseline were estimated by forcing it through the sets of  $\varepsilon$  and  $t$  (time, day) at the start and end of the curve, and by forcing the slope at the start of the curve. The start slope was determined by the slope of the light attenuation data in the 20 h before disturbance.

Recovery rate after perturbation ( $\lambda$ , per day) was defined by an exponential model:

$$\frac{d\varepsilon}{dt} = -\lambda(\varepsilon_0 - \varepsilon_c)$$

where  $\varepsilon_0$  is the light attenuation coefficient of the baseline and  $\varepsilon_c$  is the light attenuation of the chemostat (both m<sup>-1</sup>). We calculated  $\lambda$  by a linear regression of  $-\ln(\varepsilon_0 - \varepsilon_c)$  against time. To avoid the effect of the light data correction for sensor position (Supplementary Note 2), recovery rates were calculated only on the first 18–20 h after perturbation. In this period there was no change in light meter position. Finally, the recovery rates were linearly regressed against incoming light intensity.

**Autocorrelation and variance.** Autocorrelation and variance of the continuous small fluctuations in our time series were analysed for each uninterrupted period between the daily manipulations and light increments. We performed all analyses on untransformed data (5-min averages of light attenuation data) as well as on data that were averaged over non-overlapping periods of 30 min. We removed the trends from each period with a constant light level by fitting polynomials of 2 degrees to the light attenuation, and we used the residuals to calculate the autocorrelation by fitting an autoregressive model of lag 1 and variance by estimating sample variance per day.

We analysed the effect of measurement noise using a null model (see Supplementary Notes 4).

- Huisman, J. & Weissing, F. J. Light-limited growth and competition for light in well-mixed aquatic environments: an elementary model. *Ecology* **75**, 507–520 (1994).

## Supplementary Notes 1. A Mathematical Model of the System.

We modelled our cyanobacterial monoculture by applying the simple formulation of Huisman (1997)<sup>1</sup>. Primary production is integrated over the water column while accounting for self-shading by cyanobacterial biomass. The gross growth rate increases with light intensity under low light conditions, but decreases under high light conditions due to photoinhibition. We modelled the density  $A$  of a monoculture growing in a water column of depth  $z$  as:

$$\frac{dA}{dt} = p_{\max} \left( \frac{1}{z} \int_0^z P(I) dz \right) A - lA \quad (1)$$

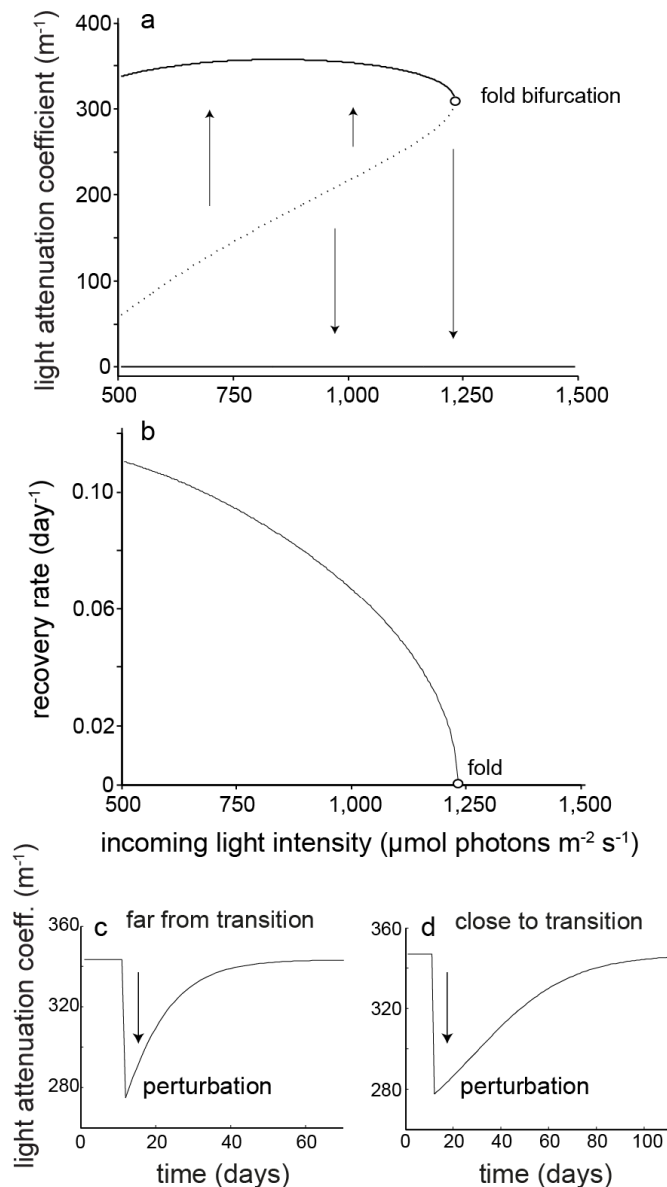
where  $p_{\max}$  is the maximum growth rate of the monoculture,  $l$  is the loss rate due to processes such as respiration, death, or dilution, and  $P(I)$  is the gross production rate as a function of the light intensity integrated over the whole water column and averaged over depth. The specific function of gross production as a function of light we used is:

$$P(I) = \frac{I}{aI^2 + I + hA} \quad (2)$$

where light intensity  $I$  is given by the Lambert-Beer law ( $I(z) = I_{in} e^{(-kA - k_{bg})z}$ ) with  $I_{in}$  the incoming light intensity,  $k$  the light attenuation coefficient and  $k_{bg}$  the background turbidity<sup>2</sup>. We used parameter values that correspond roughly to the parameterization of our experiment ( $P_{\max}=0.65 \text{ day}^{-1}$ ,  $l=0.2 \text{ day}^{-1}$ ,  $a=0.055 \text{ } \mu\text{mol photons}^{-1} \text{ m}^2 \text{ s}$ ,  $hA=100 \text{ } \mu\text{mol photons m}^{-2} \text{ s}^{-1}$ ,  $k_{bg}=10 \text{ m}^{-1}$ ,  $z_{\max}=0.01 \text{ m}$ ,  $k=1 \text{ m}^2/\text{g}$ ). By setting the vertical light attenuation per biomass of phytoplankton ( $k$ ) to 1, we express population density in units of vertical light attenuation, making comparison with our experiment easier.

In this model, cyanobacterial biomass increases with light intensity until it reaches a fold bifurcation where photoinhibition leads to the collapse of the cyanobacterial population<sup>1,2</sup> (Supplementary Fig. 1.1a). The eigenvalue of the cyanobacterial population is predicted to approach zero smoothly over the range of light values used in our experiment (Supplementary Fig. 1.1b). As a result the recovery from a perturbation is slower close to the bifurcation (Supplementary Fig. 1.1d) than further away from it (Supplementary Fig. 1.1c).

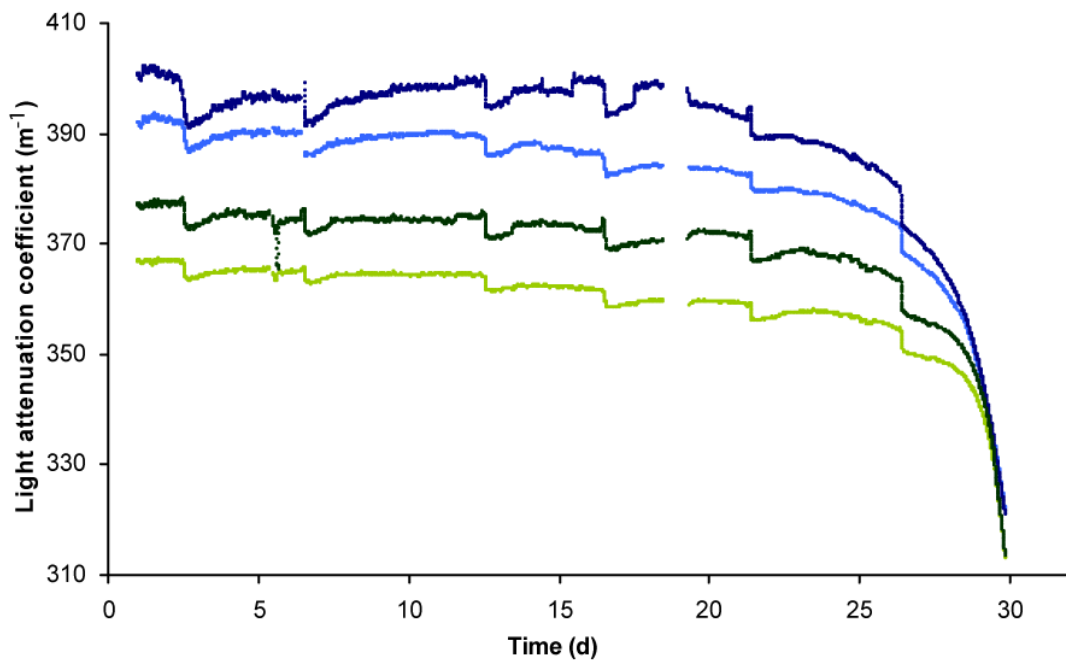
The model was solved numerically in MATLAB 7.6 with the software package GRIND (<http://www.aew.wur.nl/UK/GRIND>) using an Euler integration scheme with a step of 0.02 day.



**Supplementary Figure 1.1. Critical transitions in a modelled phytoplankton population under light stress.** (a) When light reaches a threshold value an unstable equilibrium that marks the border of the basin of attraction (dashed curve) collides with the stable equilibrium (upper solid curve) in a fold bifurcation. Here, stability of the high biomass state is lost and the population will collapse. (b) Return rates to the stable state (absolute eigenvalues) go to zero as the fold bifurcation is approached. Recovery from a perturbation (by biomass removal) is faster far from the bifurcation (panel c;  $I_{in} = 550 \mu\text{mol photons m}^{-2} \text{s}^{-1}$ ) than close to the bifurcation (panel d;  $I_{in} = 1,100 \mu\text{mol photons m}^{-2} \text{s}^{-1}$ ).

**Supplementary Notes 2.** Correction of the Light Data for Light Meter Position

The outgoing light data showed small jumps at the moments of re-attachment of the light meters. These jumps were corrected by matching the average of the last five five-minute averages of the light attenuation data before removing the sensor to the first five five-minute averages of the light attenuation data after re-attaching the light sensor (Supplementary Figure 2.1).



**Supplementary Figure 2.1. Correction of the light data for differences in light meter position.** Lines indicate uncorrected (dark blue, M1; dark green M2) and corrected (light blue, M1; light green, M2) extinction coefficients of both microcosms.

**Supplementary Notes 3. Culture Conditions Under Light Stress**

Changes in chlorophyll-a concentrations and biovolumes of the cyanobacterial populations showed similar patterns as light attenuation. Microcosm 1 (M1) reached a stable light attenuation coefficient at an  $I_{in}$  of  $477 \mu\text{mol photons m}^{-2} \text{s}^{-1}$ , microcosm 2 (M2) reached a stable light attenuation coefficient at an  $I_{in}$  of  $571 \mu\text{mol photons m}^{-2} \text{s}^{-1}$ . Both cultures reached high population densities, with maximum chlorophyll-a concentrations of  $44.12 \text{ mg l}^{-1}$  for M1 and  $43.09 \text{ mg l}^{-1}$  for M2. Maximum biovolumes were  $22 \mu\text{l ml}^{-1}$  for M1 and  $15 \mu\text{l ml}^{-1}$  for M2. The cultures were not kept in a stable state, but continuously changed in growth rate due to increases in light intensity. Maximum growth rates observed during the experimental period were  $0.48 \text{ d}^{-1}$  for M1 (at an  $I_{in}$  of  $728 \mu\text{mol photons m}^{-2} \text{s}^{-1}$ ) and  $0.35 \text{ d}^{-1}$  for M2 (at an  $I_{in}$  of  $774 \mu\text{mol photons m}^{-2} \text{s}^{-1}$ ). Around an  $I_{in}$  of  $980 \mu\text{mol photons m}^{-2} \text{s}^{-1}$  for M1 and  $1210 \mu\text{mol photons m}^{-2} \text{s}^{-1}$  for M2 the cultures started to wash out, i.e. the growth rates were lower than the chemostat dilution rate. Growth rates did not drop to 0 during the experiment.

**Supplementary Notes 4. Autocorrelation and Variance as Early-Warnings in this Experiment**

**The null model for measurement noise.** Autocorrelation and variance are indirect measures of critical slowing down, which are expected to increase before a critical transition<sup>3</sup>. These indicators require a noisy variation in the conditions with a reasonably constant distribution<sup>3</sup>. This experiment was not designed to have such variation in conditions, so most variation in biomass could be attributed to measurement noise, e.g. from the light sensors. Measurement noise in light measurements translates in a nonlinear way to the vertical light attenuation through the Lambert-Beer law. We analysed the potential effect of this nonlinear translation on observed trends in variance and autocorrelation towards the tipping point by comparing the experimentally observed trends with 1000 data sets generated with a null model. In this model we assume that all variation in the measurements is uncorrelated and normally distributed measurement noise.

First, we estimated the distribution of the maximal possible measurement noise. For this we detrended the measured light intensity ( $I_{out}$ ) with a polynomial of two degrees for each uninterrupted period between the daily manipulations and light increments. The standard deviations of the residuals were indeed reasonably constant: there was only a weak positive trend in M2 (M1:  $n=23$ ,  $R^2=0.012$ ,  $P=0.617$ ; M2:  $n=23$ ,  $R^2=0.337$ ,  $P=0.004$ ). The measurement noise was assumed to be normally distributed with the average standard deviation of the residuals of each microcosm.

Then, we generated 1000 data sets by adding this measurement noise to the polynomials describing the daily trends in light intensity ( $I_{out}$ ). Subsequently, we calculated the vertical light attenuation ( $Kd$ ) from these generated data using the Lambert-Beer law. Of each of these 1000 data sets we calculated the autocorrelation and the variance in the vertical light attenuation in the same way as described in the methods. We also determined the trends in autocorrelation and variance using Pearson's correlation coefficient. We used the distributions determined with the 1000 data sets to test whether the experimentally observed autocorrelation and variance was significantly different from the null model (i.e. when they were outside the 5% and 95% percentiles of the null model). As variance generated from the null model was strongly correlated with the biomass, we corrected the variance for the estimated effects of measurement noise propagation by subtracting the median of the null model (Fig. 2d).

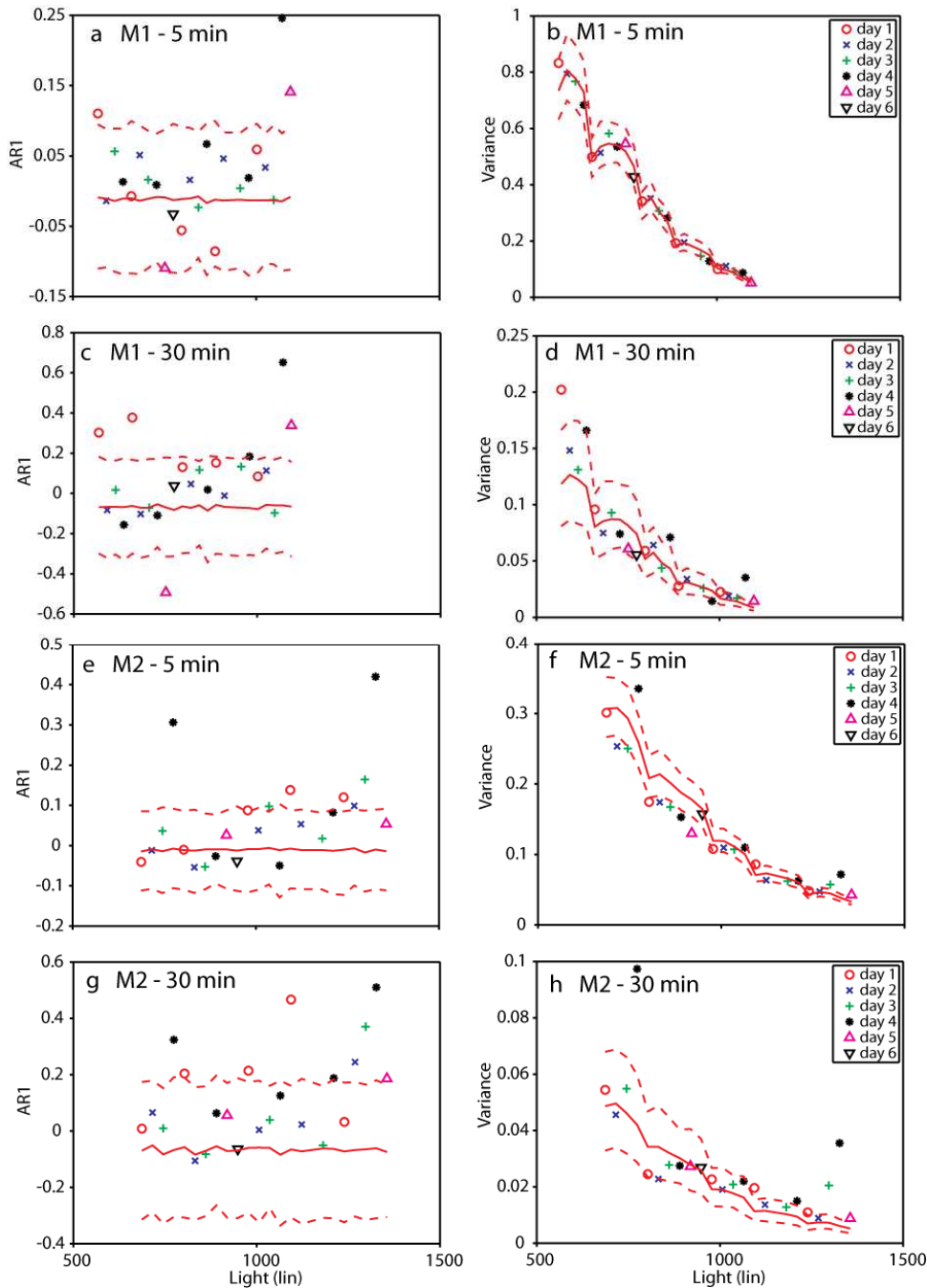
**Results.** Contrary to the expectation, the variance of the light attenuation of the microcosms decreased towards the critical transition (Supplementary Fig. 4.1). However, if we draw all variation in the system independently from a normal distribution (the null model), the variance decreases in a very similar way (percentiles in Supplementary Fig. 4.1). Therefore the decrease in variance cannot be caused by the internal dynamics, but merely by the calculation of vertical light attenuation from the measured light. During the experiment, we increased the incoming light intensities, which translated to higher outgoing light and by the Lambert-Beer law to a decrease in the variance of the vertical light attenuation. If we try to correct for this effect by subtracting the median light attenuation estimated from the null model, we have mostly no significant trend, though the observed variance is mostly significantly different from the trends calculated in the null model (Supplementary Table 4.1). Averaging over 30 minutes made the trend slightly stronger, but overall still not significant.

There was no trend in autocorrelation in the null model, so autocorrelation was less affected by measurement noise, though the variability was high (Supplementary Fig. 4.1). The trend in autocorrelation was both different from the null model and significantly positive (Supplementary Table 4.1). The result was robust for different ways of averaging the data (Supplementary Fig. 4.1).

**Supplementary Table 4.1. Trends in autocorrelation and variance.** The trends in autocorrelation and variance (as Pearson's  $\rho$  correlation coefficient) were compared with trends from 1000 runs of the null model to get an estimate of the probability that these indicators differed from the null model. Linear regressions were performed to test how autocorrelation and variance were related to incoming light intensity (see Fig. 2 of the main text).

	<b>M1</b> <b>No averaging</b>	<b>M1</b> <b>30 minutes</b>	<b>M2</b> <b>No averaging</b>	<b>M2</b> <b>30 minutes</b>
<b>Autocorrelation</b>				
Null model ( $\rho$ )	0.295 ( $p < 0.09$ )	0.361* ( $p < 0.05$ )	0.444* ( $p < 0.02$ )	0.431* ( $p < 0.03$ )
Regression ( $R^2$ )	0.087 ( $p < 0.17$ )	0.130 ( $p < 0.09$ )	0.197* ( $p < 0.03$ )	0.186* ( $p < 0.04$ )
<b>Variance</b>				
Null model ( $\rho$ )	-0.97 ( $p < 0.89$ )	-0.88* ( $p < 0.05$ )	-0.90 ( $p < 0.99$ )	-0.64 ( $p < 0.99$ )
Regression ( $R^2$ )**	0.007 ( $p < 0.69$ )	0.10 ( $p < 0.12$ )	0.19* ( $p < 0.04$ )	0.011 ( $p < 0.61$ )

\*= significant ( $p < 0.05$ ); \*\*= corrected with the median of the null model.



**Supplementary Figure 4.1. Autocorrelation and variance in both microcosms** compared with probability distributions based on 1000 runs of the null models where fluctuations were assumed to be entirely due to uncorrelated measurement noise. The dashed lines are the 5 and 95% percentiles of the model runs and the solid lines represent the medians. Different markers indicate the number of days after a perturbation. a,b) Microcosm 1, raw data (each 5 minutes); c,d) Microcosm 1 data averaged in non-overlapping periods of 30 minutes; e,f) Microcosm 2, raw data; g,h) Microcosm 2 data averaged over 30 minutes.

### Supplementary References

- 1 Gerla, D. J., Mooij, W. M. & Huisman, J. Photoinhibition and the assembly of light-limited phytoplankton communities. *Oikos* **120**, 359-368 (2011).
- 2 Huisman, J. *The struggle for light*, University of Groningen, (1997).
- 3 Scheffer, M. *et al.* Early-warning signals for critical transitions. *Nature* **461**, 53-59 (2009).